Scientific
Research

Spectroscopy and Optical Properties of Sm³⁺:YAG Nanocrystalline Powder Prepared by Co-Precipitation Method: Effect of Sm³⁺ Ions Concentrations

Hanan Ali, Maram T. H. Abou Kana, Mohamed Atta Khedr

Department of Laser Sciences and Interactions, National Institute of Laser Enhanced Sciences, University of Cairo, Giza, Egypt
Email: makdr@yahoo.com

Abstract

Samarium doped Yttrium aluminum garnet (YAG) nanopowders with different concentration (0.5%, 1%, 2%, 3%, 5% and 8% mol) were prepared by simple and low cost co-precipitation method. We found that the precursor begins converting to pure YAG at relatively low temperature around 900°C, and no intermediate phases were detected. The powders annealed at 900°C and 1000°C in air with average particle size around ≈30 nm were characterized by means of X-ray diffraction (XRD) analysis and infrared (IR) spectroscopy. The photoluminescent measurements showed that the reddish-orange (RO) emission transition $^4G_{5/2}$:$^6H_{7/2}$ is more prominent. In addition, the optimum concentration of doped Sm ions that lead to maximum intensity was reported. Also, fluorescence efficiencies as pumping power dependence for different Sm³⁺ ions concentrations were explored.

Keywords

Sm³⁺; YAG Nanopowders; Concentration Dependence Optical Properties; Ceramics

1. Introduction

Recently, the need for materials that combine transparency, high strength, scratch resistance, and thermal stability has driven the development of transparent ceramics for optical and laser applications [1] [2]. YTTRIUM ALUMINUM GARNET ($Y_3Al_5O_{12}$, YAG) is a synthetic crystal of complex cubic oxide, best known as laser

host material due to its excellent mechanical, thermal, and optical stabilities [3], and received considerable attention because of its interesting properties when doped with lanthanides ions such as neodymium [4], erbium, ytterbium, [5] chromium, [6] europium [7] and cerium [8] [9]. In 1995, Ikesue *et al*. [10] reported successful fabrication and laser operation of transparent Nd:YAG ceramics with optical properties nearly the same as those of single crystal. In compared to single crystal, the transparent polycrystalline ceramic formed by sintering of nanopowders becomes a good alternative because of its higher doping concentrations, low-cost, easy and short time of fabrication. The limitation in the transparent ceramic technology arises from the relativity low transmittance of incident ray which affecting the out-put power and laser efficiency [11]. Nanosized powders of single dispersion and uniform shape without agglomeration are highly demanded to achieve excellent optical and thermal homogeneities. The various fabrication techniques for transparent YAG ceramic or powder can be grouped into two classes: 1) traditional solid-state reaction methods which require repeated mechanical mixing and extensive heat treatment at temperatures of 1600˚C to achieve the desired phase purity; and 2) methods based on wet-chemistry synthesis of a precursor material that significantly lowered the crystallization temperature of YAG and improved the phase purity of the final product such as co-precipitation [12], Sol-gel [13], microwave irradiation [14], pechini synthesis [15]. However, it is still a challenge for the fabrication of RE:YAG nanopowder with desired sinterabilities and microstructures from the chemical point of view, the properties of nanopowders are affected by many factors which need to be carefully controlled such as solvents, precipitants, reaction temperature, pH values, duration of aging, and calcined temperature [3] [16]-[19].

To the best of our knowledge, there are a few reports on the optical properties of Sm:YAG nanopowders. Recently, there is growing interest in Sm^{3+} emission in red-orange region as phosphors materials. Laser action has been reported in $TbF_3:Sm^{3+}$ crystal and Sm^{3+} doped silica glass fiber [20]. Also, there is great interest in Sm:YAG as optical pressure sensors and a suppression material for the amplified spontaneous emission in Nd:YAG laser. Thus, we prepared Sm:YAG nanocrystal with co-precipitation method. The phase structure and the effects of samarium concentration on the optical properties of the prepared samples have been investigated.

2. Experimental

$Y(NO_3)_3 \cdot 6H_2O$ (99.99% sigma Alderich), $Al(NO_3)_3 \cdot 9H_2O$ (99.99% sigma Alderich), and $Sm(NO_3)_3 \cdot 6H_2O$ (99.99% sigma Alderich) were used as starting materials. Aqueous solution of Y, Al, Sm nitrates were mixed in which the molar ration of Sm:Y was controlled to (0.5%, 1%, 2%, 3%, 5%, and 8%). The molar ration of (Sm + Y):Al was kept as 3:5 in the mixed-metal nitrate solution. The precipitant solution was prepared by dissolving ammonium hydrogen carbonate (NH_4HCO_3) into distilled water (0.5 M). The chemical precipitation was performed by the reverse-strike technique (adding salt solution to the precipitant solution) at speed of 2 ml·min^{-1} accompanied by stirring at ambient temperature. After titration (pH = 7.9), the suspension was aged for 12 h, and then filtrated and washed several time with distilled water to remove residual ammonia and finally ultrasonically with ethanol. After drying the precipitant at 80˚C for 24 h a loose precursor was obtained and calcined in air for 2 h at temperature 900˚C and 1000˚C at heating rate of 10˚C min^{-1}.

The phase and size identification of YAG nanopowders were investigated by X-ray diffraction (Philips Analytical X-Ray, 0.154 nm for CuKα). The composition of the powders was recorded by the Fourier Transmission Infrared Spectroscopy (FT-IR spectrometer (Bruker, IFS 66/S) in the range (400 - 4000 cm^{-1})) over range of 400 - 4000 cm^{-1} with the KBr pellet technique. The absorption spectra were carried out with Camspec M501 single beam UV-Vis. The emission spectra were measured by spectrofluorometer (VARIAN CARY 5000). The fluorescence efficiency as pumping power dependence was performed by Diode laser (laser wave LWVL 405 nm, Model: 100555) as pumping source. The emitted light from the samples was collected and focused to the Oplenic spectrophotometer which was connected to a computer unit for processing the spectrum.

3. Result and Discussion

3.1. X-Ray

Figures 1(a) and **(b)** reveal the evolution of the X-ray diffraction pattern as a function of the calcination temperature of the precursor as well as samarium concentration. The X-ray pattern demonstrate that crystalline YAG started to form without any intermediate phase at relatively lower temperature equal 900˚C in compared to other preparation methods such as solid-state reaction (usually formed at 1500˚C - 1600˚C) [10]. This was attributed
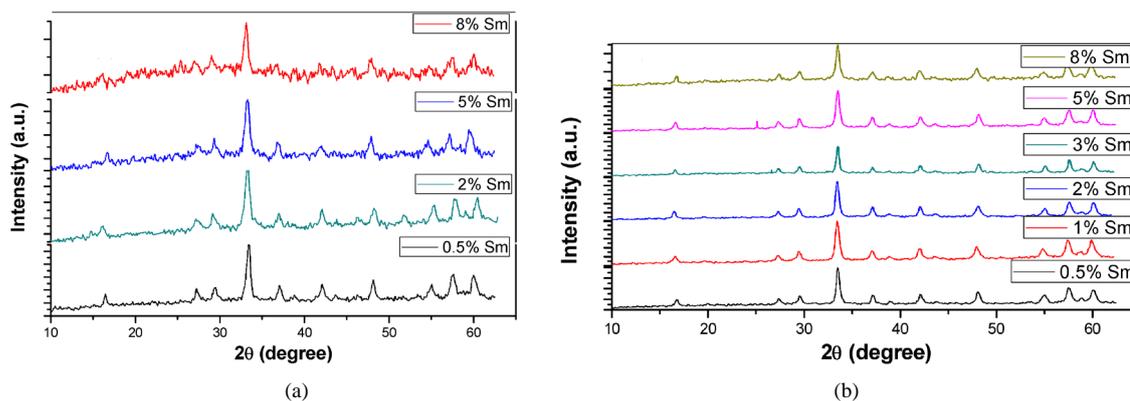
Figure 1. XRD patterns of Sm:YAG nanopowders calcinated at (a) 900°C and (b) 1000°C for different concentrations of Sm[3+] ions.

to the shorter diffusion distance for the reactants resulting from the fine grain size of the precipitated carbonate precursor [1]. Above 900°C, continued refinement of peak shapes and intensities were observed, indicating crystalline growth of the YAG powder as temperature increased. Also one can observe that, no obvious intermediate phase in YAG was observed with the increasing of Sm[3+] concentration. The average crystalline size (D) of the prepared sample at different temperature and Sm[3+] content was calculated from the broadening of the XRD (420) peak using scherrer's formula:

$$D = \frac{K\lambda}{\beta\cos\theta} \tag{1}$$

where, D the average crystalline size, K is a dimensionless shape factor, has a typical value of about 0.9, λ is the X-ray wavelength (0.154 nm for CuKα), θ is the diffraction angle, β is the peak full-line width at half maximum. The calculated crystalline size shows an increase from (23) to (46) nm as the calcination temperature increases from 900°C to 1000°C.

3.2. FT-IR

Figure 2 shows the FT-IR spectra of 2% Sm:YAG heated at 900°C and 1000°C in the range 400 - 4000 cm^{-1}. The broad absorption band peaking at around 3450 cm^{-1} is assigned to the stretching vibrations of the hydroxyl group (O-H bond) including water and Y/Al hydroxyl group, which become weaker with the increase of calcination temperature. In addition, new intense peaks in the range of 800 - 450 cm^{-1} (794, 727, 693, 569, 515 and 449 cm^{-1}) appeared. These peaks represented the characteristic metal-oxygen vibration (Al-O, Y-O, Y-O-Al) of YAG structure [11] [21]. This is evidenced by the XRD results. We also noticed that these characteristics bands as the same as in YAG single crystal [11].

3.3. Absorption Spectra

Figure 3 shows the UV-Visible absorption spectrum of Sm[3+] doped YAG nanocrystal. The spectrum consists of a set of absorption peaks, which arise from intra-configurational (f-f) transition from the ground state of Sm[3+] ions ($^{6}H_{5/2}$) to various excited states. The absorption peaks could be assigned easily on the basis of [22] [23]. Moreover, almost the detected peaks exhibit no shift with increasing Sm concentrations. This is expected since in rare earth elements L-S coupling is dominant and shield the inner electrons *i.e.* we are dealing with almost free ions.

3.4. Emission Spectra

Figure 4(a) shows the room temperature emission spectra of investigated samples recorded under the 405 nm excitation wavelength calcinated at 1000°C. The fluorescence spectra reveal four well resolved bands originating from the $^{4}G_{5/2}$ excited state to the $^{6}H_{5/2}$, $^{6}H_{7/2}$, $^{6}H_{9/2}$ and $^{6}H_{11/2}$ levels [20]. Most intense lines are at 606 and
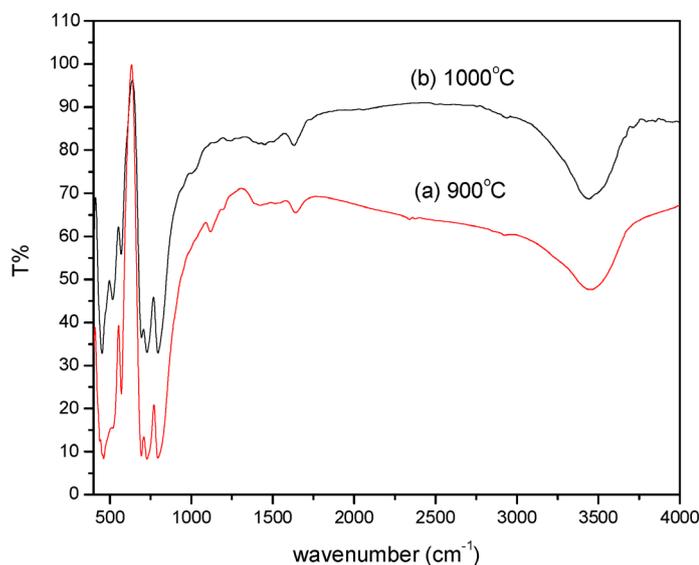
Figure 2. FT-IR spectra of 2% Sm:YAG nanopowders calcinated at (a) 900˚C and (b) 1000˚C.
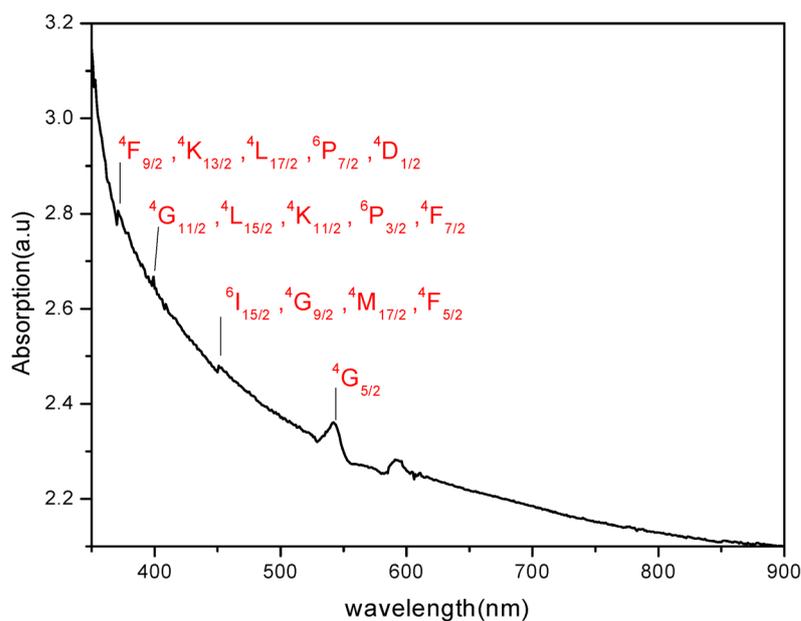

Figure 3. Absorption spectra of 2% Sm:YAG nanopowders calcinated at 1000˚C.

618 nm, because the state $^6H_{7/2}$ is split into stark energies owing to crystal field. As well as the $^4G_{5/2}$ to $^6H_{9/2}$ fluorescence band with intense line at 658 nm is dominant in spectrum, giving rise to the reddish orange emission.

We found that the fluorescence intensity increased as Sm^{3+} concentrations increased up to 2% then quenching behavior was observed. **Figure 4(b)**, compares between the maximum emission intensity of Sm:YAG nanopowders calcinated at (900˚C and 1000˚C) as a function of Sm concentration. Remarkable enhancement in the peak intensity was observed due to rising the calcination temperature in samples (0.5%, 1%, and 2%) with no change detected in the emission peaks positions. In other words, the intensity of 2% Sm was raised to double as the calcination temperature increased to 1000˚C. This may be attributed to decrease the number of defect states inside the samples due to the crystallinity improvement in case of these samples as demonstrated in X-ray.

It is worth mentioning that there is no change observed in the emission spectral band width as the Sm concentration increased which confirm that there is no secondary phase has been formed. Whereas, in other work re-

porting [12], broadening in the band width in case of Nd:YAG samples as changing the Nd ion concentration and referring it to formation of secondary phases was observed.

3.5. Fluorescence Efficiency as Input Pumping Power Dependence

Figure 5 presents the integrated PL intensity as a function of input pump power for different Sm concentrations. For fitting our data, the dependence of the PL intensity on the power of the exciting laser light can be defined by using the relation of $I \sim P^K$ [24] where I is the intensity of the luminescence and P represents the input excitation energy and K is a number with value ranging from zero to less than 1 for sublinearity relationship whereas from 1 to 2 for linear and superlinear relation. By fitting the data in figure. It was found that K value is always more than 1 which proof the superlinearity between the input excitation power and output intensity. These results indicate that the good optical properties for the samples that can be used as an active medium for laser systems. Moreover, we can observe that, the sample of 2% Sm concentration has higher slope. This mean that, at the same pumping power, the sample of 2% Sm:YAG give higher emitted photons than other samples.
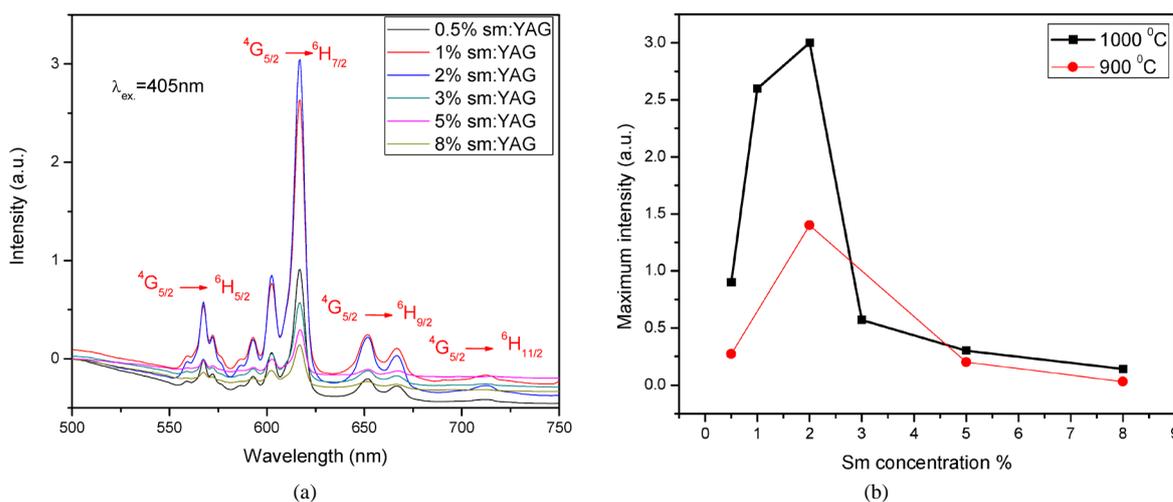

Figure 4. (a) Emission spectra of Sm:YAG nanopowders calcinated at 1000°C for different concentrations of Sm^{3+} ions, (b) Maximum integrated peak intensity for the calcinated samples (900°C and 1000°C) as a function of Sm concentration.
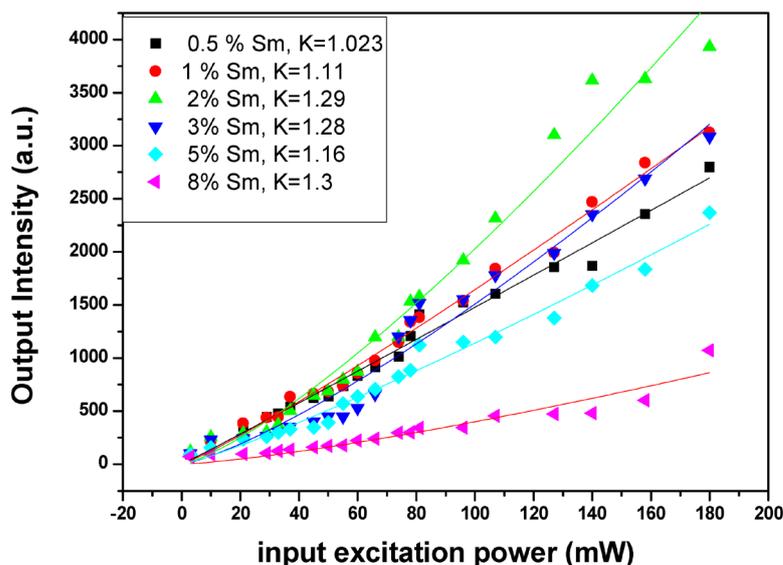

Figure 5. Input-output excitation intensity dependence for Sm:YAG nanopowder with different Sm concentrations.

4. Conclusion

Nanocrystalline Sm:YAG has been successfully synthesized by the co-precipitation method using ammonium hydrogen carbonate as a precipitant. The precursor is converted directly to pure YAG at about 900˚C. As the calcination temperature raises, the YAG particle size was found to increase from 23 to 46 nm. The photoluminescent properties of the prepared samples showed that the reddish-orange (RO) emission transition $^4G_{5/2}$:$^6H_{7/2}$ is more prominent. In addition, the optimum samarium concentration—(2%)—that leads to maximum fluorescence was recorded. The final product was found to be pure structure and uniform distributed YAG nanopowders which are anticipated to be used as the candidate for sintering transparent ceramic materials. The fluorescence efficiency as input pumping power dependence experiment shows that the sample of 2% Sm has higher slope efficiency in compared to other samples. This can be widely used in the development of LEDs and the possible applications as a laser material operating at different lines in 600 - 670 nm spectral range.

Acknowledgements

References

[1] Fedyk, R., Hreniak, D., Łojkowski, W., Stręk, W., Matysiak, H., Grzanka, E., Gierlotka, S. and Mazur, P. (2007) Method of Preparation and Structural Properties of Transparent YAG Nanoceramics. *Optical Materials*, **29**, 1252-1257. http://dx.doi.org/10.1016/j.optmat.2006.05.016

[2] Taira, T. (2007) Ceramic YAG Lasers. *Comptes Rendus Physique*, **8**, 138-152. http://dx.doi.org/10.1016/j.crhy.2006.08.002

[3] Sang, Y., Lv, Y., Qin, H., Zhang, X., Liu, H., Wang, J., Sun, X. and Boughton, R.I. (2012) Chemical Composition Evolution of YAG Co-Precipitate Determined by pH during Aging Period and Its Effect on Precursor Properties. *Ceramics International*, **38**, 1635-1641. http://dx.doi.org/10.1016/j.ceramint.2011.09.054

[4] Ikesue, A., Kamata, K. and Yoshida, K. (1996) Effects of Neodymium Concentration on Optical Characteristics of Polycrystalline Nd:YAG Laser Materials. *Journal of the American Ceramic Society*, **79**, 1921-1926. http://dx.doi.org/10.1111/j.1151-2916.1996.tb08014.x

[5] Garskaite, E., Lindgren, M., Einarsrud, M.-A. and Grande, T. (2010) Luminescent Properties of Rare Earth (Er, Yb) Doped Yttrium Aluminium Garnet Thin Films and Bulk Samples Synthesised by an Aqueous Sol-Gel Technique. *Journal of the European Ceramic Society*, **30**, 1707-1715. http://dx.doi.org/10.1016/j.jeurceramsoc.2010.01.001

[6] Ikesue, A., Yoshida, K. and Kamata, K. (1996) Transparent Cr^{4+}-Doped YAG Ceramics for Tunable Lasers. *Journal of the American Ceramic Society*, **79**, 507-509. http://dx.doi.org/10.1111/j.1151-2916.1996.tb08154.x

[7] Yang, H.K. and Jeong, J.H. (2009) Synthesis, Crystal Growth, and Photoluminescence Properties of YAG:Eu^{3+} Phosphors by High-Energy Ball Milling and Solid-State Reaction. *The Journal of Physical Chemistry C*, **114**, 226-230. http://dx.doi.org/10.1021/jp908903t

[8] Lu, C.-H. and Jagannathan, R. (2002) Cerium-Ion-Doped Yttrium Aluminum Garnet Nanophosphors Prepared through Sol-Gel Pyrolysis for Luminescent Lighting. *Applied Physics Letters*, **80**, 3608-3610. http://dx.doi.org/10.1063/1.1475772

[9] Nishiura, S., Tanabe, S., Fujioka, K., Fujimoto, Y. and Nakatsuka, M. (2009) Preparation and Optical Properties of Transparent Ce:YAG Ceramics for High Power White LED. *IOP Conference Series*: *Materials Science and Engineering*, **1**, 012031.

[10] Ikesue, A., Kinoshita, T., Kamata, K. and Yoshida, K. (1995) Fabrication and Optical Properties of High-Performance Polycrystalline Nd:YAG Ceramics for Solid-State Lasers. *Journal of the American Ceramic Society*, **78**, 1033-1040. http://dx.doi.org/10.1111/j.1151-2916.1995.tb08433.x

[11] Ge, X.-X., Sun, Y.-H., Liu, C. and Qi, W.-K. (2009) Influence of Combustion Reagent and Microwave Drying Method on the Characteristics of Nano-Sized Nd^{3+}:YAG Powders Synthesized by the Gel Combustion Method. *Journal of Sol-Gel Science and Technology*, **52**, 179-187. http://dx.doi.org/10.1007/s10971-009-2013-3

[12] Saladino, M.L. and Caponetti, E. (2009) Co-Precipitation Synthesis of Nd:YAG Nanopowders II: The Effect of Nd Dopant Addition on Luminescence Properties. *Optical Materials*, **32**, 89-93. http://dx.doi.org/10.1016/j.optmat.2009.06.008

[13] Lu, C.-H., Hong, H.-C. and Jagannathan, R. (2002) Sol-Gel Synthesis and Photolumine-Scent Properties of Cerium-Ion

Doped Yttrium Aluminium Garnet Powders. *Journal of Materials Chemistry*, **12**, 2525-2530.
http://dx.doi.org/10.1039/b200776m

[14] Vaidhyanathan, B. and Binner, J.G.P. (2006) Microwave Assisted Synthesis of Nanocrystalline YAG. *Journal of Materials Science*, **41**, 5954-5957. http://dx.doi.org/10.1007/s10853-006-0260-z

[15] Galceran, M., Pujol, M.C., Aguiló, M. and Díaz, F. (2008) Synthesis and Characterization of Nanocrystalline Yb:Lu$_2$O$_3$ by Modified Pechini Method. *Materials Science and Engineering*: *B*, **146**, 7-15.
http://dx.doi.org/10.1016/j.mseb.2007.07.038

[16] Zhang, X., Liu, D., Sang, Y., Liu, H. and Wang, J. (2010) Effects of Aging on the Characteristics of Nd:YAG Nano-Powders. *Journal of Alloys and Compounds*, **502**, 206-210. http://dx.doi.org/10.1016/j.jallcom.2010.04.144

[17] Li, J.-G., Ikegami, T., Lee, J.-H., Mori, T. and Yajima, Y. (2000) Co-Precipitation Synthesis and Sintering of Yttrium Aluminum Garnet (YAG) Powders: The Effect of Precipitant. *Journal of the European Ceramic Society*, **20**, 2395-2405. http://dx.doi.org/10.1016/S0955-2219(00)00116-3

[18] Katelnikovas, A., Barkauskas, J., Ivanauskas, F., Beganskiene, A. and Kareiva, A. (2007) Aqueous Sol-Gel Synthesis Route for the Preparation of YAG: Evaluation of Sol-Gel Process by Mathematical Regression Model. *Journal of Sol-Gel Science and Technology*, **41**, 193-201. http://dx.doi.org/10.1007/s10971-006-9002-6

[19] Yang, L., Lu, T., Xu, H., Zhang, W. and Ma, B. (2010) A Study on the Effect Factors of Sol-Gel Synthesis of Yttrium Aluminum Garnet Nanopowders. *Journal of Applied Physics*, **107**, 064903. http://dx.doi.org/10.1063/1.3341012

[20] Malinowski, M., Wolski, R., Frukacz, Z., Lukasiewicz, T. and Luczynski, Z. (1995) Spectroscopic Studies of YAG:Sm^{3+} Crystals. *Journal of Applied Spectroscopy*, **62**, 840-843. http://dx.doi.org/10.1007/BF02606647

[21] Gong, H., Tang, D.-Y., Huang, H. and Ma, J. (2009) Agglomeration Control of Nd:YAG Nanoparticles via Freeze Drying for Transparent Nd:YAG Ceramics. *Journal of the American Ceramic Society*, **92**, 812-817.
http://dx.doi.org/10.1111/j.1551-2916.2009.02987.x

[22] Lin, H., Yang, D., Liu, G., Ma, T., Zhai, B., An, Q., Yu, J., Wang, X., Liu, X. and Yue-Bun Pun, E. (2005) Optical Absorption and Photoluminescence in Sm^{3+}- and Eu^{3+}-Doped Rare-Earth Borate Glasses. *Journal of Luminescence*, **113**, 121-128. http://dx.doi.org/10.1016/j.jlumin.2004.09.115

[23] Mahato, K.K., Rai, D.K. and Rai, S.B. (1998) Optical Studies of Sm^{3+} Doped Oxyfluoroborate Glass. *Solid State Communications*, **108**, 671-676. http://dx.doi.org/10.1016/S0038-1098(98)00442-6

[24] Schmidt, T., Lischka, K. and Zulehner, W. (1992) Excitation-Power Dependence of the Near-Band-Edge Photoluminescence of Semiconductors. *Physical Review B*, **45**, 8989-8994. http://dx.doi.org/10.1103/PhysRevB.45.8989